The Journal of Experimental Biology 214, 848-857

doi:10.1242/jeb.051276

RESEARCH ARTICLE

The protective role of aquaporins in the freeze-tolerant insect *Eurosta solidaginis*: functional characterization and tissue abundance of EsAQP1

Benjamin N. Philip[1,2,*], Andor J. Kiss[1] and Richard E. Lee, Jr[1]

[1]Laboratory for Ecophysiological Cryobiology, Department of Zoology, Miami University, 700 East High Street, Oxford, OH 45056, USA and [2]Department of Biology, Rivier College, 420 S. Main Street, Nashua, NH 03060, USA

*Author for correspondence (bphilip@rivier.edu)

Accepted 8 November 2010

SUMMARY

The movement of water and small solutes is integral to the survival of freezing and desiccation in insects, yet the underlying mechanisms of these processes are not fully known. Recent evidence suggests that aquaporin (AQP) water channels play critical roles in protecting cells from osmotic damage during freezing and desiccation. Our study sequenced, functionally characterized and measured the tissue abundance of an AQP from freeze-tolerant larvae of the gall fly, *Eurosta solidaginis* (Diptera: Tephritidae). The newly characterized EsAQP1 contains two NPA motifs and six transmembrane regions, and is phylogenetically related to an AQP from the anhydrobiotic chironomid *Polypedilum vanderplanki*. Using a *Xenopus laevis* oocyte swelling assay, we demonstrated that EsAQP1 increases water permeability to nine times that of simple diffusion through the membrane. In contrast to its high water permeability, EsAQP1 was impermeable to both glycerol and urea. The abundance of EsAQP1 increased from October to December in all tissues tested and was most abundant in the brain of winter larvae. Because the nervous system is thought to be the primary site of freezing injury, EsAQP1 may cryoprotect the brain from damage associated with water imbalance. The sequence, phylogenetic relationship, osmotic permeability, tissue distribution and seasonal abundance of EsAQP1 further support the role of AQPs in promoting freezing tolerance.

Supplementary material available online at http://jeb.biologists.org/cgi/content/full/214/5/848/DC1

Key words: EsAQP1, cold tolerance, acclimation, osmotic stress, water balance, *Xenopus* swelling assay.

INTRODUCTION

Organisms that experience excessive shifts in solute concentration and water distribution during osmotic challenge risk sustaining structural damage to their cells and/or disruption of proper cell function (Hadley, 1994). One adaptation that is well known to protect cells against the osmotic challenges of freezing and desiccation is the accumulation of low molecular weight compounds, such as glycerol, urea and trehalose (Ring and Danks, 1994). In preparation for winter, some insects amass multi-molar levels of these molecules, which colligatively reduces the rate of ice formation and the amount of ice that develops (Lee, 1991; Lee, 2010). In addition, these compounds decrease the rate of water loss and serve as molecular substitutes for water during dehydration (Ring and Danks, 1994).

Recently, aquaporins (AQPs) have also been implicated in protecting cells against osmotic damage [see Borgnia et al. and Campbell et al. (Borgnia et al., 1999; Campbell et al., 2008) and references therein]. These proteins, which are water-selective, transmembrane channels found in both prokaryotic and eukaryotic cells, act as conduits for rapid water flux ($\sim 3\times10^9$ water molecules subunit^{-1} cell^{-1}) greatly exceeding simple diffusion across the membrane (Borgnia et al., 1999; Preston et al., 1992). During freezing, concentration gradients build between the intracellular and extracellular fluid compartments, when water becomes osmotically inactive as ice. As the extracellular concentration of solutes increases, intracellular water must rapidly leave the cell to alleviate the increasing osmotic pressure and prevent damage to the membrane (Mazur, 1984; Muldrew et al., 2004). Linking AQPs to this rapid redistribution of water may ultimately provide another dimension to our understanding of adaptations for freeze tolerance and survival of osmotic stress.

Cells of freeze-tolerant organisms must simultaneously coordinate the efflux of water and influx of cryoprotectants, such as glycerol, in response to the concentration of extracellular solutes during ice formation. Aquaglyceroporins (GLPs), a subgroup of AQPs permeable to water and small uncharged solutes (Borgnia et al., 1999), are implicated in the cellular movement of glycerol during freezing (Izumi et al., 2006; Philip and Lee, 2010; Philip et al., 2008; Zimmerman et al., 2007). The importance of glycerol uptake through GLPs in freezing survival is suggested by the improved cryopreservation survival of mouse oocytes that artificially express GLPs (Edashige et al., 2003). The ability of AQPs and GLPs to redistribute molecules may also explain why the rate of freezing can influence the survival of insects (Bale et al., 1989) and frogs (Costanzo et al., 1991). During rapid freezing, the rate of ice formation may simply overwhelm the cell's ability to redistribute water and cryoprotectants effectively through AQPs and GLPs. The role of these proteins in water and low molecular weight solute movement, as well as their ability to allow cells to rapidly respond to osmotic stress, suggests that AQPs and GLPs play a significant role in protecting cells during freezing.

One organism that naturally survives freezing is the goldenrod gall fly, *Eurosta solidaginis* (Baust and Nishino, 1991). Larvae of these flies are exposed to environmental extremes as they overwinter inside the stem of goldenrod (*Solidago* spp.) (Layne, 1993). Northern populations experience temperatures as low as –40°C within their galls (Baust and Lee, 1981). Consequently, *E. solidaginis* have developed the remarkable capacity to withstand extreme winter conditions; fully freeze-tolerant larvae can survive exposure to –80°C (Bennett and Lee, 1997; Philip and Lee, 2010). As such, *E. solidaginis* serves as an excellent model organism not only to investigate natural adaptations to freezing but also to potentially provide insight for the clinical cryopreservation of mammalian tissues.

Our previous study demonstrated that tissues from *E. solidaginis* are unable to survive freezing in the presence of an AQP/GLP inhibitor (Philip et al., 2008). This result suggests a critical role for AQPs/GLPs in facilitating water exosmosis and/or cryoprotectant (e.g. glycerol) uptake during freezing. To further our understanding of their role in meeting osmotic challenges, we isolated, cloned and sequenced an AQP from *E. solidaginis* and functionally characterized its water and solute permeability. Additionally, we investigated the abundance of this AQP among different tissues during seasonal cold-hardening in *E. solidaginis* larvae. The functional characterization and observed changes in seasonal protein abundance for this AQP provide further evidence that these proteins are important in promoting freeze tolerance.

MATERIALS AND METHODS

Insect collection

Spherical galls containing the larvae of *E. solidaginis* (Diptera: Tephritidae), Fitch 1855, were collected from goldenrod plants (*Solidago* sp.) near Oxford, OH, USA, including at the Miami University Ecology Research Center (39°31′57″N, 84°43′23″W). Larvae were collected in late October (2007) for cDNA cloning, and early October and late December (2007) for immunoblots. Larvae for immunoblots were snap-frozen and stored at –80°C.

cDNA cloning of aquaporins

Larvae were homogenized in Ultraspec RNA isolation reagent (Biotecx, Houston, TX, USA). The poly(A)$^+$ mRNA fraction was isolated from the total RNA using oligo(dT)-cellulose (Biotecx) following standard protocols (Sambrook and Russell, 2001). cDNA was synthesized from mRNA using the Reverse Transcriptase System (Promega, Madison, WI, USA). The cDNA was reverse transcribed with a cDNA cloning primer (cDNA cloning primer: 5′-GGCCACGCGTCGACTAGTACTTTTTTTTTTTTTTTV-3′, Integrated DNA Technologies, Coralville, IA, USA) and used in subsequent PCR amplifications.

PCRs were carried out using degenerate primers [MIP/NOD (F): 5′-GG(GATC)G(GC)(GATC)CA(TC)(TCA)T(GATC)AA(TC)C-C(GATC)GC(GATC)GT(GATC)AC-3′; MIP/NOD (R): 5′-C(TG)(GATC)GC(GATC)GG(AG)TTCAT(GATC)(GC)(ATC)(G-ATC)GC(GATC)CC(GATC)GT-3′] designed to conserved regions of AQP sequences (Elvin et al., 1999). Thermocycler conditions were: 94°C for 2 min with 40 cycles of 94°C for 1 min, 50°C for 1 min, 72°C for 1 min. The ends of the amplicon were finished during a final incubation at 72°C for 10 min. All reactions were analyzed by agarose gel electrophoresis; bands between 400 and 500 base pairs were excised, processed using Wizard SV Gel and PCR Clean-Up System (Promega), and subcloned into a pGEM-T Easy vector (Promega) as per the manufacturer's instructions. Vectors were transformed into JM109 competent cells (Promega) and white colonies were selected for by α-complementation of LacZ on LB plates containing 100 μg ml^{-1} ampicillin supplemented with IPTG and X-gal. White, insert-containing colonies were grown in 4 ml of LB media (containing 100 μg ml^{-1} ampicillin) overnight and plasmid DNA was isolated using Wizard SV Minipreps DNA Purification System (Promega) and sequenced using a BigDye Terminator v3.1 cycle sequencing kit (Applied Biosystems, Foster City, CA, USA) and standard T7 or SP6 sequencing primers (Promega). Products were analyzed on an Applied Biosystems 310 or 3130× DNA Sequencer in the Center for Bioinformatics and Functional Genomics at Miami University.

Complete cDNA sequences were obtained by 5′ and 3′ rapid amplification of cDNA ends (RACE). The 3′ RACE forward primer was complementary to the putative AQP (EsAQP1 3′ RACE primer: 5′-GGCGGGGCGTGTAAGCGTTTTGCGTGCC-3′) and the reverse primer (3′ RACE PCR: 5′-GGCCACGCGTCGAC-TAGTAC-3′; Integrated DNA Technologies) corresponded to the cDNA cloning primer. This method yielded the remainder of the 3′ end, as well as the untranslated region (UTR). 5′ RACE was performed on terminal deoxynucleotidyl transferase (TdT)-tailed cDNA [EsAQP1 5′ RACE (F): 5′-GGCCACGCGTCGA-CTAGTACGGGIIGGGGIGGGIIG-3′, EsAQP1 5′ RACE (R): 5′-GCCCAAATGACCGAGGGTGACAGAGAGACCGATGGC-GAG-3′] to obtain the previously unidentified 5′ end of the AQP. The entire sequence was amplified with a gene-specific forward primer [EsAQP1 Whole Sequence (F): 5′-GCAAGCAATTT-CACGAGAAGCTTATTAAATTTAAAACACTGCCGG-3′] and the 3′ RACE PCR reverse primer, and was cloned into a pGEM-T Easy vector. The rat AQP3 plasmid was constructed from RNA isolated from rat kidneys, using rat AQP3 forward (5′-GCCTCGCCATGGGTCGACAGAAGGAG-3′) and reverse (5′-GCATCACAAGGGGGCTTTATGGGGTGTCCC-3′) primers based on Edashige et al. (Edashige et al., 2003). Human AQP1 plasmid (Preston et al., 1992) was a generous gift of Prof. Peter Agre (The Johns Hopkins University, Baltimore, MD, USA). Human AQP1 was used as a positive control for the water permeability assay and rat AQP3 was used as a positive control for both the water and glycerol permeability assays.

Analysis of sequences

DNA sequences were edited for quality and aligned by ClustalW in BioEdit 7.0.9.0 (Hall, 1999). *In silico* translated aquaporin cDNAs from *E. solidaginis* were compared by BLASTp with GenBank at NCBI. Amino acid analysis was carried out using BioEdit 7.0.9.0. Hydropathy plots (http://ca.expasy.org/tools/protscale.html) (Kyte and Doolittle, 1982) were constructed to predict the number of membrane-spanning regions, as well as to make comparisons to known aquaporins from GenBank/NCBI. For the predicted transmembrane regions, we evaluated the primary structure regions using TMHMM Server, V. 2.0 (http://www.cbs.dtu.dk/services/TMHMM/) as well as structural comparisons at ExPaSy SwissModel (http://swissmodel.expasy.org/). Based on these results, we constructed a two-dimensional membrane topology plot using the T_EXtopo package (Beitz, 2000) and employed a group of selected, aligned aquaporins for the purpose of shading *via* the T_EXshade package. Based on the alignment, individual amino acids were shaded if the majority of the residues had similar characteristics ('similar'), the majority were the same residue ('conserved'), or all residues were identical ('invariable') at a particular location. Putative phosphorylation and glycosylation sites were identified by ScanProsite (http://expasy.org/tools/scanprosite/) (De Castro et al., 2006) on the ExPaSy server.

A three-dimensional analysis of structural conservation among AQPs was performed with the structural alignment of multiple proteins (STAMP) tool within the Visual Molecular Dynamics (VMD) program (Humphrey et al., 1996). Residues were colored based on their *Q*-value, with blue assigned to structurally conserved regions and red to sites with no correspondence in structure.

Phylogenetic analysis of the putative *E. solidaginis* AQP was performed by Bayesian analysis using aligned amino acid sequences of insects and selected taxa for which functional data have been published (supplementary material Table S1). Nucleotide sequences were aligned based on a ClustalX amino acid alignment using a codon-constraint approach implemented by CodonAlign2.0 (Hall, 2004). Analysis was performed using PAUP4.0*b10 and MrBayes 3.1.2. Tree construction was done by MrBayes 3.1.2 using a 'Generalised Time Reversible plus Invariant plus Gamma' (GTR+I+Γ) evolutionary model (Waddell and Steel, 1997) as selected by MrModeltest v2.3 (Nylander, 2004). Four runs using four chains and 10,000,000 generations were performed. All other parameters in MrBayes 3.1.2 were left at default. Stationarity was assessed using the 'sump burnin=2500' command and by examining the plot of the generation *versus* the log likelihood values. A 50% majority rule consensus tree was generated using the command 'sumpt burnin=2500'. A newick tree file, including branch lengths and Bayesian consensus values, was imported into the tree explorer of MEGA4 (Kumar et al., 2008) to draw the phylogram.

Xenopus oocyte swelling assay

Before cRNA for oocyte injections was transcribed, a fragment of the *Xenopus* β-globin 5′-UTR was subcloned into the pGEM-T Easy plasmid, downstream of the T7 promoter site and upstream of the ATG start site, as described in detail elsewhere (Zimmerman et al., 2007). This step was necessary because our preliminary swelling assays suggested that proteins were not translated efficiently by *Xenopus* oocytes when the cRNA did not contain the *Xenopus* β-globin 5′-UTR fragment. EsAQP1 and rat AQP3 plasmids were linearized with *Spe*I and cRNA was synthesized with the mMessage mMachine T7 kit (Applied Biosystems) as described by the manufacturer. Human AQP1 was linearized with *Sma*I and cRNA was synthesized with the mMessage mMachine T3 kit (Applied Biosystems). cRNA was treated with TURBO DNase (Applied Biosystems), recovered with a phenol:chloroform extraction and ethanol precipitation, and resuspended in RNase-free water. The cRNA from each reaction was verified on a denaturing agarose gel to contain only a single product, then aliquoted and frozen at –80°C.

Ovaries from double-pithed, mature female *Xenopus laevis* frogs were removed according to a protocol approved by the Institutional Animal Care and Use Committee at Miami University (Protocol 750). The tissue was minced into small pieces using fine forceps and treated with 2 mg ml^{-1} collagenase A (Roche, Mannheim, Germany) in Ca^{2+}-free modified Barth's solution (Ca^{2+}-free MBS; 88 mmol l^{-1} NaCl, 1 mmol l^{-1} KCl, 2.4 mmol l^{-1} $NaHCO_3$, 10 mmol l^{-1} Hepes, 0.82 mmol l^{-1} $MgSO_4$, pH 7.5) for 3 h at 15°C with gentle agitation. Oocytes were washed repeatedly with fresh MBS (Ca^{2+}-free MBS with 0.33 mmol l^{-1} $Ca(NO_3)_2$, 0.41 $CaCl_2$; 177 mOsm) to remove residual collagenase, and Stage V and VI oocytes were incubated overnight at 15°C in MBS containing 10 mg l^{-1} gentamicin. Any follicular layers that remained attached were manually removed from oocytes using fine forceps and oocytes were injected (Nanoject II, Drummond, Broomall, PA, USA) with either 50.6 nl of 500 ng μl^{-1} cRNA recovered from the mMessage mMachine reactions or the same volume of RNase-free water. Oocytes were incubated in MBS containing 10 mg l^{-1} gentamicin for 3 days (with daily changes of media) at 15°C before being used in swelling assays.

To assay water permeability, oocytes were placed in diluted (hypotonic) MBS solution (63 mOsm) at room temperature, and images were taken with a Nikon D300 (Tokyo, Japan) camera attached to an Olympus SZX12 (Tokyo, Japan) microscope every 20 s for 3 min, or until the oocyte burst. The cross-sectional area of the oocytes was measured with Image Pro 6.3 (Media Cybernetics, Bethesda, MD, USA) and used to calculate relative volume (V/V_0) as $V/V_0=(A/A_0)^{3/2}$, where A and A_0 are the cross-sectional areas of the oocyte at time t and 0, respectively. The osmotic water permeability coefficient (P_f), which was the mean of 8–10 oocytes, was determined using the volume of the oocyte at time 0 (V_0), the initial rate of change in the relative volume of the oocytes [$d(V/V_0)/dt$] between the time points of 20 and 40 s during the hypotonic challenge, the initial oocyte surface area (S), the molar volume of water (V_w; 18 cm^3 mol^{-1} or 0.018 l mol^{-1}) and the osmotic gradient (Osm_{in}–Osm_{out}), with the following equation (Zhang and Verkman, 1991):

$$P_f = [V_0 \times d(V/V_0)/dt] / [S \times V_w \times (Osm_{in} - Osm_{out})] . \quad (1)$$

To examine whether mercury is inhibitory to these AQPs, a subset of oocytes (N=6) were incubated in 0.3 mmol l^{-1} $HgCl_2$ for 10 min before hypotonic challenge in (Hg^{2+}-free) diluted MBS. To determine whether mercury inhibition was reversible, another group of oocytes (N=5) were incubated in 0.3 mmol l^{-1} $HgCl_2$ for 10 min followed by 15 min in 5 mmol l^{-1} β-mercaptoethanol (BME), a reducing agent.

Apparent glycerol and urea permeability were assayed volumetrically by measuring changes in oocyte volume (N=5–8) following their placement into isosmotic MBS containing 165 mmol l^{-1} glycerol or urea substituted for 88 mmol l^{-1} NaCl. This method tests whether these AQPs are permeable to these solutes by measuring the response of water to glycerol and urea concentration gradients. If glycerol or urea diffuses into the oocyte through solute-permeable AQPs, the medium becomes hypotonic and water will move into the cell in response to the concentration gradient. Therefore, only oocytes that contain AQPs permeable to these solutes will swell (Echevarria et al., 1996; Kataoka et al., 2009). The solute permeability ($P_{sol}\times10^{-6}$ cm s^{-1}) was calculated using the equation:

$$P_{sol} = [d(V/V_0)/dt] / [V_0/S] , \quad (2)$$

with the change in relative volume between oocyte measurements taken at 20 and 40 s into the experiment.

Immunoblots

To determine the abundance of EsAQP1 protein in tissues, larvae that had been collected in October and December and immediately frozen at –80°C were thawed and quickly dissected. Fat body, gut, Malpighian tubule, salivary gland and brain were removed and placed on ice in protein isolation medium (250 mmol l^{-1} sucrose and 10 mmol l^{-1} triethanolamine adjusted to pH 7.6 with 1 mol l^{-1} NaOH) containing Protease Inhibitor Cocktail (Sigma P8340; 1:100 dilution). Each tissue type was pooled (N=4 individuals) and proteins were extracted by grinding tissues with a Teflon pestle and sonicating the solution. Homogenates were centrifuged (4°C) for 10 min at 1000 ***g*** to remove large cellular debris, the protein concentration of the supernatants (whole protein fractions) was determined with a Bradford assay (BioRad, Hercules, CA, USA) and 3 μg of protein were analyzed through immunoblotting and densitometry techniques described previously (Philip and Lee, 2010). A polyclonal rabbit EsAQP1 antibody was developed using a peptide corresponding to the C-terminus of the predicted EsAQP1

protein (Cys-KYRTHADDREMRKLDSTRDYA) (Proteintech, Chicago, IL, USA). Rabbit serum was affinity purified and used in immunoreactions at a final concentration of 0.5 μg ml^{-1} in TBS-T containing 5% non-fat milk. The specificity of this and other primary antibodies was characterized by probing *Xenopus* oocytes expressing either EsAQP1 or rat AQP3. Oocyte proteins were isolated in media containing 20 mmol l^{-1} Tris-HCl, pH 7.6, 0.1 mol l^{-1} NaCl and 1% Triton X-100 (Bossi et al., 2007) with protease inhibitors (Sigma; 1:100 dilution). Isolates from EsAQP1- and rat AQP3-expressing oocytes were probed with EsAQP1, rat AQP3 (Sigma A0303, 1:300 dilution) or rat AQP4 (Sigma A5971, 1:1000 dilution) primary antibodies.

Statistics

Changes in relative volume within each group of AQP-injected oocytes during the swelling assay are plotted as means ± 1 s.e.m. Water (P_f) and solute (P_{sol}) permeabilities among different AQPs were compared using an ANOVA and Bonferroni–Dunn *post hoc* test.

RESULTS

Isolation, cloning, sequencing and phylogenetic analysis of EsAQP1

We isolated, cloned and sequenced a partial cDNA of an AQP from *E. solidaginis* using degenerate primers designed against conserved regions of AQPs. The full sequence (1305 bp), including the UTRs, was obtained through 5′ and 3′ RACE (GenBank accession no. FJ489680). *In silico* translated cDNA revealed that this new AQP possesses two aspargine–proline–alanine (NPA) amino acid motifs (Fig. 1A). A Kyte–Doolittle hydropathy plot (supplementary material Fig. S1) suggests there are six transmembrane regions connected by five loops, such that the N- and C-termini are located in the cytosol. Two-dimensional topology of this novel AQP showed the locations of the transmembrane regions, the NPA motifs and putative post-translational modification sites (Fig. 1B). Predicted cytosolic casein kinase II (Thr 251, Ser 263) and protein kinase C (Ser 246, Ser 263) phosporylation sites and an extracellular N-glycosylation (Asn–Ile–Thr–Glu 132) site are indicated on the diagram (Fig. 1B).

The phylogenetic relationship of this *E. solidaginis* aquaporin to functionally characterized AQPs from human (*Homo sapiens sapiens*), quail (*Coturnix coturnix*), Cope's gray tree frog (*Hyla chrysoscelis*), Mozambique tilapia (*Oreochromis mossambicus*), vinegar fly (*Drosophila melanogaster*), yellow fever mosquito (*Aedes aegypti*), mulberry silkworm moth (*Bombyx mori*), green leafhopper (*Cicadella viridis*), triatomid bug (*Rhodnius prolixus*), sleeping chironomid (*Polypedilum vanderplanki*), pea aphid (*Acyrthosiphon pisum*), brown dog tick (*Rhipicephalus sanguineus*), nematode roundworm (*Caenorhabditis elegans*) and *Escherichia coli* was determined by Bayesian analysis (see supplementary material Table S1 for GenBank accession numbers). The outgroup in our phylogram was a bacterial aquaporin (*E. coli* AQPZ). A phylogram based on the Bayesian analysis is presented as a 50% majority rule consensus tree in Fig. 2. The evolutionary model indicated as most suitable by MrModelTest (Nylander, 2004) was the GTR+I+Γ model of substitution. In this analysis, we used codon-constrained nucleotide alignments of the coding regions of the aquaporins (supplementary material Fig. S2). The newly sequenced *E. solidaginis* AQP is most closely related to the dehydration-inducible *P. vanderplanki* AQP1 (PvAQP1), to which it is 52.3% identical at the amino acid level. Based on its identity and phylogenetic relationship to PvAQP1, we designated this AQP cloned from *E. solidaginis* as EsAQP1. Both EsAQP1 and PvAQP1 are ancestral to a clade of AQPs in organisms ranging from insects to mammals. According to this phylogenetic reconstruction, EsAQP1 is distantly related to GLPs from both human (HsAQP3) and Cope's gray tree frog, *H. chrysoscelis* (HcAQP3). The alignment of the EsAQP1 amino acid sequence to the most closely related insect (PvAQP1) and human (HsAQP4) AQPs using ClustalW (BLOSUM62) demonstrated high homology among the three proteins, especially near the NPA motifs (Fig. 1). The predicted three-dimensional structures of EsAQP1, PvAQP1 and humanAQP4 were compared using the VMD program to determine whether the amino acid differences affected the overall structure of the proteins. Areas of high structural conservation, as predicted by the *Q*-values, predominated in the transmembrane helices (Fig. 1C). In contrast, the extracellular connecting loops were more structurally divergent, as demonstrated by the prevalence of red residues (Fig. 1C).

Functional characterization of EsAQP1

Although the amino acid sequence, alignments, thread-through modeling and phylogenetic analysis suggested that EsAPQ1 was an aquaporin, it was important to confirm this prediction by functionally characterizing the water and solute permeability of this protein. We measured water permeability by translating exogenous AQPs in *Xenopus* oocytes and exposing the cells to a hypotonic challenge. Oocytes translating EsAQP1 cRNA responded to hypotonic extracellular fluid by rapidly swelling (Fig. 3; see supplementary material Movies 1–4), thereby demonstrating the protein's permeability to water. The mean osmotic water permeability coefficient (P_f) for EsAQP1 using Eqn 1 was more than 9-fold that of sham-injected oocytes ($P<0.0001$; Fig. 4A). Despite this, EsAQP1 demonstrated only 57% of the water permeability of human AQP1 ($P<0.0001$; Fig. 4A).

Exposure to mercury-containing compounds, including $HgCl_2$, inhibits water transport in most AQP isoforms, as these molecules are thought to covalently bond to the AQP channel and occlude molecular movements through the pore (Preston et al., 1993). Mercury sensitivity of EsAQP1 was demonstrated by a significant decrease in water permeability following exposure to mercuric chloride ($P<0.0001$; Fig. 4B). Generally, mercury inhibition of an AQP can be partially or totally reversed if the oocytes are exposed to a reducing agent, such as BME (Preston et al., 1993). Despite an increase in water permeability of mercury-inhibited EsAQP1 oocytes after exposure to BME, this change was not statistically significant (as measured by the conservative Bonferroni–Dunn *post hoc* test; $P=0.035$; Fig. 4B).

In addition to permitting water flux, GLPs are a subset of AQPs that permit small, uncharged solutes, such as glycerol or urea, to pass through the plasma membrane. Apparent uptake, as measured by changes in oocyte volume in response to glycerol- or urea-containing isosmotic media, was not significantly different from that of sham-injected oocytes in either experiment ($P>0.05$; Fig. 5). In contrast, rat AQP3 oocytes serving as a positive control, swelled because of their permeability to glycerol and urea (Fig. 5) (Borgnia et al., 1999).

Tissue distribution and seasonal abundance of EsAQP1

After characterizing the molecular structure and physiological function of EsAQP1, we examined the tissue-level translation of this protein. The predicted amino acid sequence for EsAQP1 was used to design a polyclonal antibody against an antigenic portion of the AQP corresponding to amino acids 248–268 on the C-terminus. To verify the antibody reacted with EsAQP1, we probed

protein isolated from EsAQP1 and rat AQP3 cRNA-injected *Xenopus* oocytes and found that the EsAQP1 antibody only reacted with EsAQP1 proteins (Fig. 6A). Immunoblots probed with the EsAQP1-specific antibody resulted in a single band at 25 kDa, which is slightly lower than the *in silico* predicted molecular mass of 29 kDa. Additionally, proteins isolated from EsAQP1 cRNA-injected *Xenopus* oocytes did not cross-react with commercially available rat AQP3 and rat AQP4 antibodies (Fig. 6A).

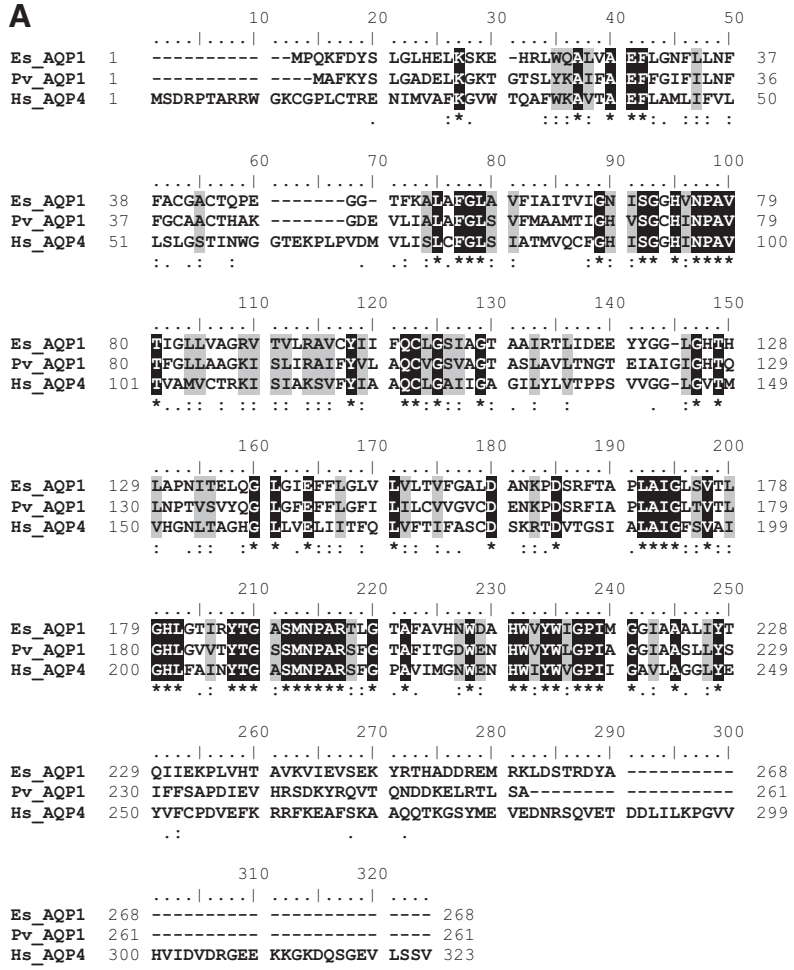

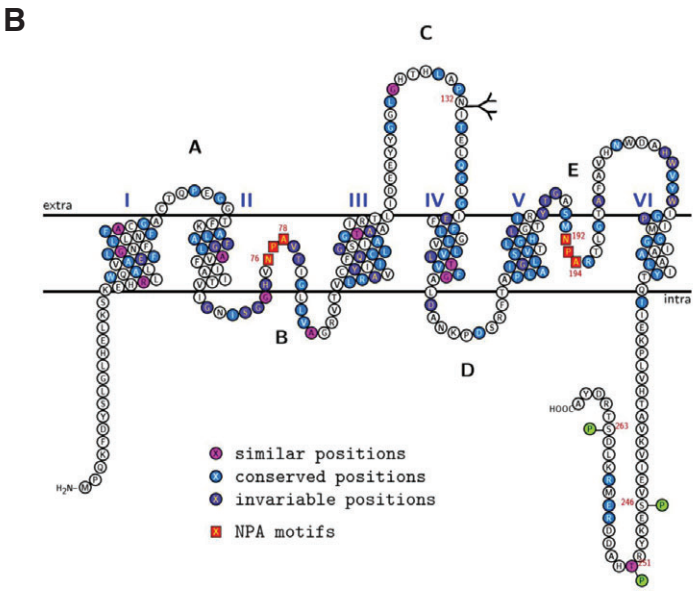

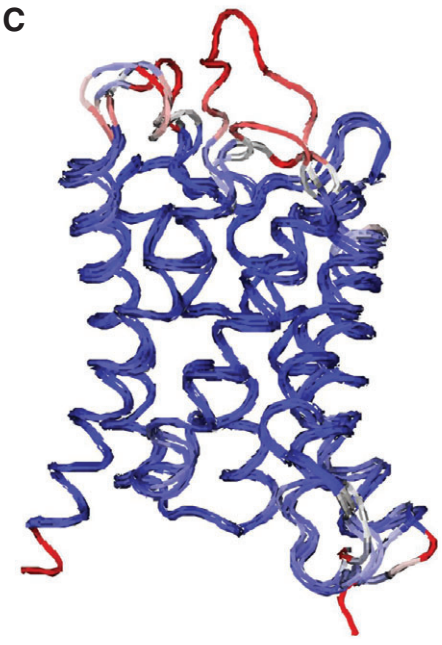

Fig. 1. Sequence of the newly identified *Eurosta solidaginis* aquaporin (AQP), EsAQP1, in relationship to other AQPs. (A) The deduced amino acid sequence of EsAQP1 demonstrates well conserved regions with both *Polypedilum vanderplanki* AQP1 (Pv_AQP1) and *Homo sapiens* AQP4 (Hs_AQP4) when aligned with ClustalW (BLOSUM62) in BioEdit v7.0.9.0. EsAQP1 is 52.3% identical to *P. vanderplanki* AQP1 and 27.8% identical to *H. sapiens* AQP4 at the amino acid level. Black boxes (*) signify identical and gray boxes (: or .) highlight conserved amino acids among all three sequences. A two-dimensional transmembrane topology plot (B) for EsAQP1 amino acids, showing the six transmembrane regions (I–VI) connected by five loops (A–E), predicts intracellular C- and N-terminal regions. Additionally, the two half-loops each contain the conserved NPA motif (red squares). Similar (pink circle), conserved (blue circle) and invariable (purple circle) residues among a subset (see supplementary material Table S1) of functionally characterized invertebrate, avian and mammalian AQPs are shown. Additionally, putative cytosolic phosphorylation (green circle) and extracellular N-glycosylation (branch) sites are indicated. The three-dimensional ribbon model (C) of EsAQP1, PvAQP1 and human AQP4 demonstrating structural conservation using the structural alignment of multiple proteins (STAMP) tool within the Visual Molecular Dynamics (VMD) program, shows that the majority of conserved regions (blue) are found in the membrane-spanning region. In contrast, the connecting loops of these proteins are more likely to have no structural conservation (red).

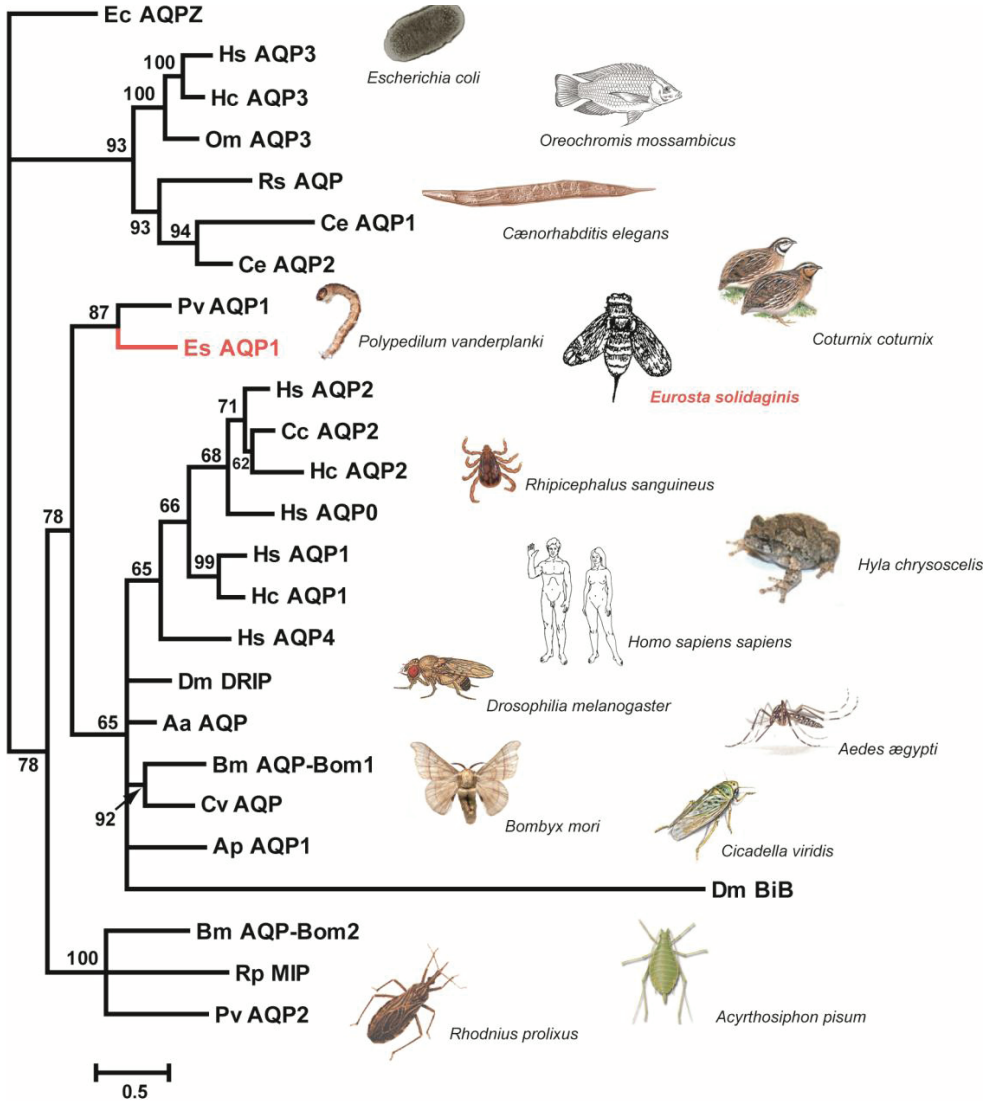

Fig. 2. Phylogram demonstrating the relationship between functionally characterized AQPs from a diverse group of invertebrate and vertebrate organisms (see supplementary material Table S1 for species list). The tree was constructed from the aligned nucleotides of the coding region from the cDNAs (supplementary material Fig. S2). The 50% majority-rule consensus tree was generated by the program MrBayes, implementing a GTR+I+Γ evolutionary model. The newly characterized *E. solidaginis* (EsAQP1) is highlighted in red. Numbers at branch points are Bayesian consensus values and the scale bar indicates 0.5 expected changes per site. Names are abbreviated as a two letter genus and species abbreviation and an AQP name/number (e.g. EsAQP1). Images of species used are included (but are not shown to scale).

The newly characterized antibody to EsAQP1 was used to assay differences in the abundance of EsAQP1 in fat body, gut, Malpighian tubule, salivary gland and brain during the cold and desiccation hardening that occurs between October and December (Fig. 6B). When standardized to total protein content, the abundance of EsAQP1 was highest in the brain. The Malpighian tubules had the next most abundant amount of EsAQP1, albeit 6-fold less than levels found in brain. When the same tissues were examined in late December, there was an overall increase in the abundance of EsAQP1 in the tissues assayed (Fig. 6B), including a nearly 4-fold increase in abundance of EsAQP1 in the salivary gland.

DISCUSSION

Surviving osmotic challenge requires the regulation and maintenance of water and solute balance between body compartments. AQPs, which rapidly redistribute water and certain small solutes across the membrane, are associated with the physiological response to stresses that require the management of cellular water, such as anhydrobiosis (Kikawada et al., 2008), feeding on osmotically challenging foods (Le Caherec et al., 1996; Shakesby et al., 2009) and survival of freezing (Izumi et al., 2006; Philip et al., 2008; Philip and Lee, 2010). To better understand the role of these proteins in osmotic stress, we identified, functionally characterized the water permeability and determined the tissue distribution of an AQP during seasonal cold acclimation in *E. solidaginis*.

Sequence and phylogenetic analysis of EsAQP1

We determined that a novel *E. solidaginis* AQP, EsAQP1, was similar in sequence, predicted topology and function to previously identified and reported AQPs (Campbell et al., 2008). This novel sequence contained two NPA motifs, six membrane-spanning regions and five connecting loops, all hallmarks of AQP proteins (Fig. 1). Additionally, the amino acids predicted to make the ar/R (aromatic/arginine) selectivity filter in PvAQP1 (Phe 56, His 181, Arg 196) (Kikawada et al., 2008) were in nearly identical positions in EsAQP1 (Phe 56, His 180, Arg 195).

Sequence comparisons among different AQPs can indicate their relationship to each other and suggest how the proteins have evolved. Alignments of EsAQP1 at both the nucleotide and amino acid levels with other functionally characterized AQPs indicate it shares a high percentage of identity with PvAQP1 from the sleeping chironomid *P. vanderplanki* (Fig. 1A). The closest human ortholog to EsAQP1 was AQP4, with an identity of 27.8% at the amino acid level (Fig. 2). EsAQP1, PvAQP1 and human AQP4 shared transmembrane regions that are well conserved, especially near the pore-forming residues of the NPA motifs (Fig. 1A,C). In contrast, both the N- and C-termini

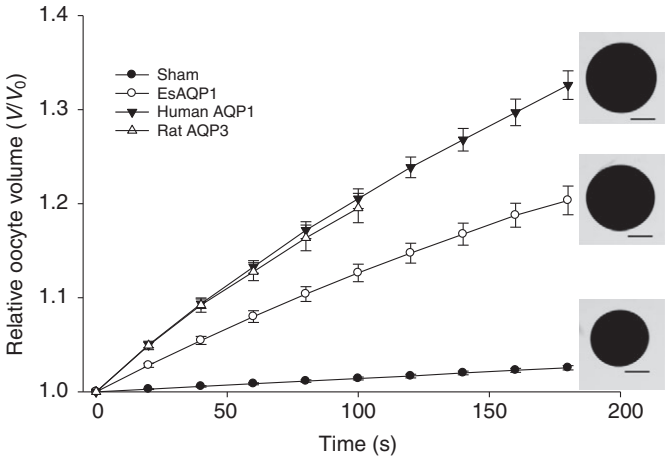

Fig. 3. The relative volume of AQP-expressing oocytes following exposure to hypotonic media was measured to characterize the osmotic permeability of these AQPs. Prior to the assay, oocytes were injected with 50 nl of AQP cRNA (500 ng μl^{-1}) or water. Results are reported as means ± s.e.m. (*N*=8–10 oocytes). The volume of each oocyte was measured for 180 s or until it burst. The relative volume of rat AQP3 oocytes is only shown over a period of 100 s, as few oocytes from the group remained intact thereafter. Inset images are (from bottom to top) single intact sham, EsAQP1 and human AQP1 oocyte at 180 s of exposure to hypotonic media (scale bars, 500 μm).

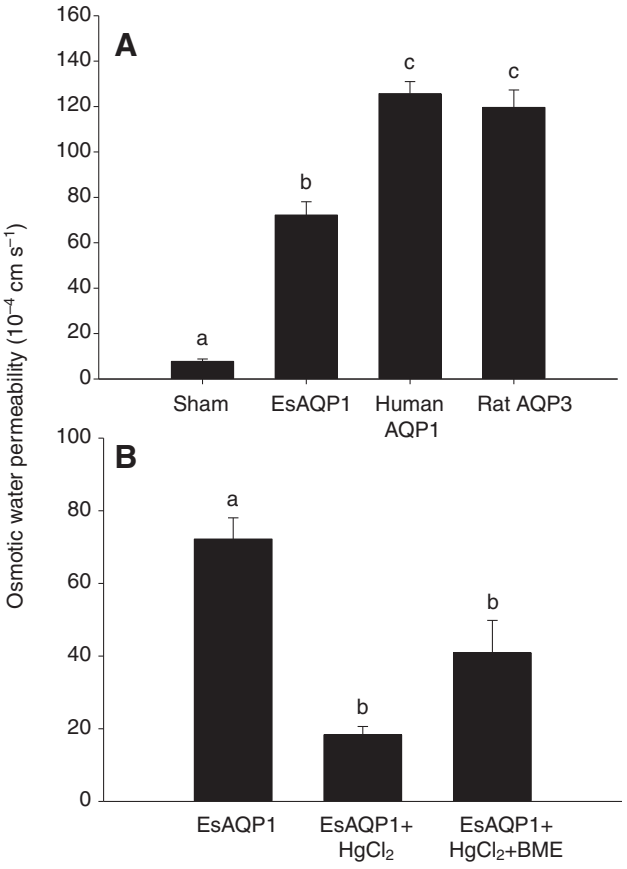

Fig. 4. The mean osmotic water permeability coefficient (P_f) for each AQP calculated from individual oocyte measurements made at 20 and 40 s into the swelling assay. (A) Oocytes (*N*=8–10) were exposed to hypotonic media and swelling was measured. Sham oocytes were injected with water, and human AQP1 and rat AQP3 served as the positive controls for this experiment. (B) The water permeability of EsAQP1 oocytes (EsAQP1; *N*=10) was compared with the permeability of oocytes following exposure to $HgCl_2$ (0.3 mmol l^{-1}) for 10 min (EsAQP1+$HgCl_2$; *N*=6). Additionally, the reversal of mercury inhibition was tested by placing oocytes in β-mercaptoethanol (BME, 5 mmol l^{-1}) for 15 min before exposure to hypotonic media (EsAQP1+$HgCl_2$+BME; *N*=5). Values are means + s.e.m. Different letters denote a significant difference between values within the same plot (a: $P<0.0083$, b: $P<0.0167$).

were more divergent among these three AQPs, suggesting these regions are under less selective pressure. Although amino acid changes in the N- and C-termini do not directly change the functional transmembrane pore, these alterations can have significant regulatory effects on the aquaporin. *Drosophila melanogaster* BIB, a member of the AQP family, has a C-terminus that is ~10-fold longer than that of 'traditional' AQPs and contains many targets for tyrosine kinase regulation (Campbell et al., 2008). Although EsAQP1 does not have an extended C-terminus, we predicted several putative phosphorylation sites that could enable functional regulation of EsAQP1 during physiological processes (Fig. 1B). These putative sites and their potential role remain to be elucidated in further regulatory studies, which are currently underway.

Despite the existence of a large number of AQP isoforms among diverse forms of life, these proteins are highly conserved. Phylogenetic analysis of EsAQP1 and a representative group of other functionally characterized AQPs was performed using Bayesian methodology and a GTR+I+Γ model of molecular evolution (Waddell and Steel, 1997). This model of evolution is particularly well suited for ancient, conserved protein-coding sequences, as it takes into account the possibility of sequence reversion, as well as the likelihood of invariant sites and the recognition that not all sites will be under the same selective pressure. Additionally, using nucleotides that code for amino acids constrained in the alignment as triplet codons likely facilitates much greater depth of resolution in phylogenetic reconstructions (Simmons et al., 2002). The clade of EsAQP1 and PvAQP1 is intriguing because, unlike many of the other organisms in the phylogenetic tree, both insects are tolerant of extreme environmental conditions. Larvae of *P. vanderplanki* can survive exposure to extreme cold (–270°C) and heat (102°C) (Hinton, 1960), and have a dehydration-inducible AQP (PvAQP1) that is presumed to facilitate rapid water loss during entry into anhydrobiosis (Kikawada et al., 2008). In addition to EsAQP1, we analyzed the partial sequence from another *E. solidaginis* AQP cDNA and found it was most closely related to another AQP of *P. vanderplanki* (PvAQP2; data not shown). Accordingly, the close phylogenetic relationship of these AQP proteins from two insects that experience similar osmotic challenges suggests that evolutionary pressures drive adaptations at the molecular level to promote organismal tolerance of extreme stress.

Functional characterization of EsAQP1

Water permeability measurements through artificial expression of AQPs in *Xenopus* oocytes provided evidence that EsAQP1 is a functional water channel. It should be noted that the rate of water flux was lower in EsAQP1 than in both human AQP1 and rat AQP3 (Fig. 4A). While EsAQP1 may naturally possess below-average water permeability, other factors could explain its reduced water flux rates. One such explanation is a change in the amino acid sequence of EsAQP1 from an ancestral protein. A substitution that changes an alanine (A) to a valine (V) in one of the normally conserved NPA motifs is thought to contribute to low water permeability in a *R.*

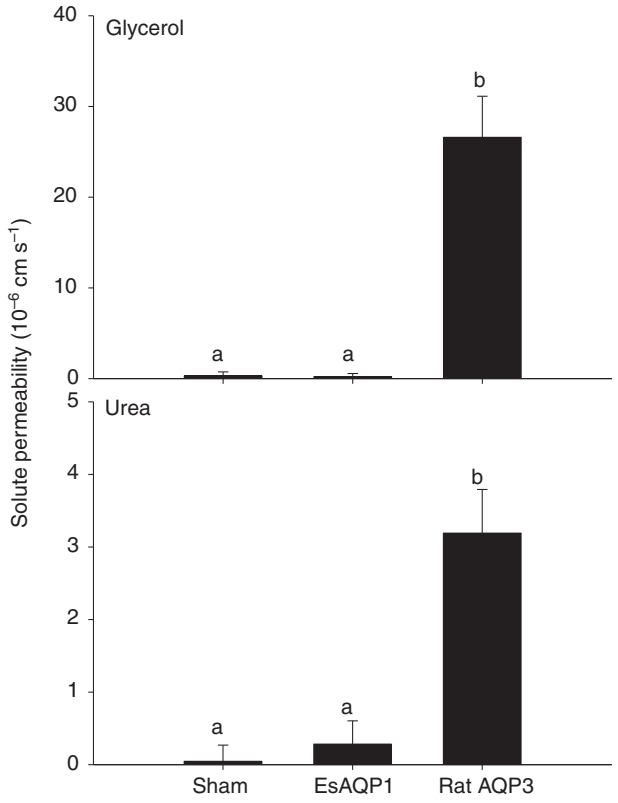

Fig. 5. Glycerol and urea permeability in sham, EsAQP1 and rat AQP3 oocytes placed in solute-substituted isotonic media. If the AQPs were permeable to the glycerol or urea, the solutes would diffuse into the oocyte, and water would follow, resulting in swelling of the oocyte. The oocyte volume was measured between 20 and 40 s into the swelling assay, and used to calculate the solute permeability coefficient. Values are means + s.e.m. for *N*=5–8 oocytes. Different letters denote a significant difference (P<0.0167) between values within the same plot.

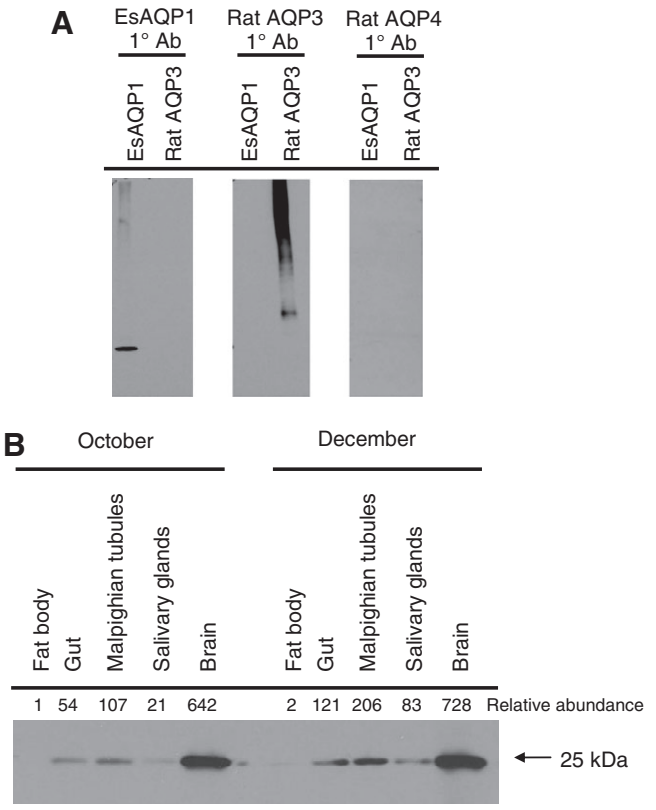

Fig. 6. The abundance of EsAQP1 in different tissues during cold hardening was assessed using immunoblots. (A) To confirm the specificity of antibodies (Ab) used to identify AQPs, EsAQP1 and rat AQP3 proteins were probed to verify they did not cross-react with other antibodies. (B) Immunoblots of fat body, gut, Malpighian tubule, salivary gland and brain from *E. solidaginis* collected in October and December were pooled from four individuals and probed with the EsAQP1-specific primary (1°) antibody. Relative protein abundance was calculated using the density and size of each band, with October fat body values set to 1.

prolixus AQP (Rp-MIP) (Echevarria et al., 2001). Although this particular substitution does not explain the reduction in permeability of EsAQP1, which contains two NPA motifs, an amino acid substitution(s) elsewhere in the protein could alter its water transport abilities. Changes to residues outside the active site of proteins can still impact their activity, as demonstrated by a single amino acid substitution altering the kinetic properties of lactate dehydrogenase A in barracudas (Holland et al., 1997). Another possible cause of the relatively lower permeability of EsAQP1 is the non-native environment in which it was tested. The permeability of some AQPs is based on post-translational modifications in response to environmental signals, such as temperature (Azad et al., 2004). If similar cues are required by EsAQP1, we may be unintentionally influencing its permeability by expressing the proteins in *Xenopus* oocytes. Understanding the mechanism by which EsAQP1 is regulated *in vivo* may provide valuable insight into the mechanism by which this protein functions in *E. solidaginis*.

Survival of freezing requires cells to exchange both water and cryoprotectants between intracellular and extracellular compartments. The permeability of AQP/GLPs to these molecules implicates these proteins in protecting against freeze-induced damage in a range of organisms, including yeast (Tanghe et al., 2002), insects (Izumi et al., 2006; Philip et al., 2008) and amphibians (Zimmerman et al., 2007). The ability of EsAQP1 channels to redistribute water across the membrane faster than by simple diffusion through membrane, as shown by our *in vitro* assay (Fig. 4), would facilitate cellular dehydration that is caused by the formation of concentrated extracellular fluid during freezing. Therefore, we predict that EsAQP1 is similar to other AQP/GLPs, and serves as a pathway for water flux to dissipate osmotic pressures across the membrane during freezing.

In addition to their important role in protecting cells against the rapid development of osmotic gradients during freezing, AQPs appear to be regulated during exposure to desiccating conditions in insects (Kikawada et al., 2008; Philip and Lee, 2010). During the autumn, the microhabitat of *E. solidaginis* becomes highly xeric as the water content of the surrounding gall tissue decreases to ~20% (Rojas et al., 1986). While the protective mechanism of AQPs during exposure to desiccating conditions is not known, these proteins, including EsAQP1, may serve as a pathway by which water movement between body compartments is controlled.

Cells not only need to rid themselves of excess water during freezing but also must accumulate cryoprotectants to protect the conformation of proteins (Carpenter and Crowe, 1988) and membrane structure (Karow, 1991) against osmotic extremes. Because glycerol is an important cryoprotectant in *E. solidaginis*, we tested whether EsAQP1 provided a pathway for its flux across the membrane. Our experimental evidence demonstrated that

EsAQP1 is impermeable to glycerol (Fig. 5), and therefore we suggest another AQP isoform is responsible for the movement of this cryoprotectant during larval freezing. Based on previous studies, which identified multiple AQP- and GLP-like proteins in *E. solidaginis* (Philip et al., 2008; Philip and Lee, 2010), and the putative number of AQPs existing in insect genomes [seven in *Drosophila* spp. and five in mosquito (Campbell et al., 2008)], EsAQP1 is likely only one of several AQP/GLP isoforms involved in glycerol and/or water redistribution during osmotic challenge.

Tissue distribution and seasonal abundance of EsAQP1

The diverse physiological functions and osmotic requirements among different tissues result in differential expression of AQP isoforms (Borgnia et al., 1999). Using an antibody against EsAQP1 to determine its distribution at the tissue level in *E. solidaginis*, we found it was most abundant in the brain. In contrast, the few studies that have functionally characterized arthropod AQPs found a relatively low abundance in the brain or head (Ball et al., 2009; Shakesby et al., 2009). AQPs in mammalian brains are critically important in regulating water movement (Tait et al., 2008); AQP4 is the most abundant AQP in the brain, where it is thought to prevent edema by eliminating excess water from brain parenchyma (Papadopolous and Verkman, 2007). In a study comparing AQP4-null and wild-type mice, application of a frozen probe to the surface of the brain resulted in more severe edema in the AQP4-null mice (Papadopolous et al., 2004). The authors concluded that the freeze injury caused the blood–brain barrier to become leaky, thereby allowing water to accumulate around the brain. Because the AQP4-null mice were unable to void excess water through AQP4, they developed damagingly high intracranial pressure. Similar to mammals, insects possess a blood–brain barrier that prevents hemolymph from directly contacting their nervous tissue and disrupting the highly regulated ionic composition of the microenvironment surrounding the neurons (Carlson et al., 2000; Chapman, 1971). If the integrity of the insect blood–brain barrier is compromised through similar mechanisms during freezing, they too would experience an accumulation of water in their nervous tissue. Damage to the nervous system is a leading candidate to explain organismal death following freezing injury in *E. solidaginis* (Collins et al., 1997); therefore, we propose the abundance of EsAQP1 in brain protects by mediating rapid dissipation of water that accumulates during freezing.

As the fat body is one of the most cold-hardy tissues in *E. solidaginis* (Bennett and Lee, 1997), we did not expect EsAQP1 to be virtually absent from this tissue (Fig. 6B). Because the fat body of *E. solidaginis* is tolerant of intracellular freezing (Lee et al., 1993), and has an intrinsically low water content (i.e. <35%) (Davis and Lee, 2001), one could argue this tissue does not require EsAQP1 in high abundance for rapid redistribution of water during freezing. Although this is a plausible explanation, the results from previous studies suggest that AQPs and/or GLPs are present in fat body, as this tissue loses its ability to tolerate freezing when frozen in the presence of an AQP inhibitor (Izumi et al., 2006; Philip et al., 2008). Furthermore, fat body is the site of glycerol biosynthesis (Kukal et al., 1988), which likely necessitates a high abundance of GLPs. Therefore, we suggest that AQPs are important to the fat body in *E. solidaginis*; however, the active AQP isoform(s) is not EsAQP1.

Seasonal cold hardening of *E. solidaginis* occurs gradually through the autumn to prepare larvae for the cold and dry winter. During this period, larvae accumulate cryoprotectants (Morrissey and Baust, 1976), enter diapause (Irwin et al., 2001) and remodel the fatty acid composition of their membranes (Bennett et al., 1997). Because *E. solidaginis* AQPs promote freeze tolerance (Philip et al., 2008) and are implicated in seasonal cold hardening (Philip and Lee, 2010), we expected to observe an increase in the abundance of EsAQP1 in tissue from October to December. The abundance of EsAQP1 increased in all surveyed tissues during this cold-hardening period (Fig. 6B). By increasing the number of AQPs, cells likely improve their ability to rapidly redistribute water, and can better protect themselves against the build-up of osmotic pressures across the membrane during freezing in winter.

The results from the current study, in which we determined the sequence, phylogenetic relationship, osmotic permeability, tissue distribution and seasonal abundance of EsAQP1, complement our previous studies that link AQPs to the other mechanisms promoting freezing tolerance in *E. solidaginis* (Philip et al., 2008; Philip and Lee, 2010). Similar to natural freeze tolerance, successful clinical cryopreservation demands rapid water efflux and cryoprotectant influx during the freezing process. Although there have been a few attempts to enhance cryopreservation success by modifying AQP abundance (Edashige et al., 2003; Tanghe et al., 2002), this approach has not resulted in greater overall success in freezing tissues and organs. Therefore, studying natural systems in which the challenges of surviving freezing have been solved at the organismal level may uncover important details concerning AQPs/GLPs that could improve clinical cryopreservation in the future.

ACKNOWLEDGEMENTS

We thank Masaaki Azuma, Hitoshi Morita and Naoto Ueno for assistance with the *Xenopus* assay, Yoshinori Tomoyasu and Matt Duley for their technical expertise, Peter Agre for the human AQP1 plasmid, David Linz for his assistance in constructing the rat AQP3 plasmid, and Jon Costanzo, Paul James, Gary Lorigan, Michael Robinson and two anonymous reviewers for comments on an earlier draft of this manuscript. This research was supported by NSF grant no. IOS-0840772 to R.E.L.

REFERENCES

Azad, A. K., Sawa, Y., Ishikawa, T. and Shibata, H. (2004). Phosphorylation of plasma membrane aquaporin regulates temperature-dependent opening of tulip petals. *Plant Cell Physiol.* **45**, 608-617.

Bale, J. S., Hansen, T. N., Nishino, M. and Baust, J. G. (1989). Effect of cooling rate on the survival of larvae, pupariation and adult emergence of the gall fly *Eurosta solidaginis*. *Cryobiology* **26**, 285-289.

Ball, A., Campbell, E. M., Jacob, J., Hoppler, S. and Bowman, A. S. (2009). Identification, functional characterization and expression patterns of a water-specific aquaporin in the brown dog tick, *Rhipicephalus sanguineus*. *Insect Biochem. Mol. Biol.* **39**, 105-112.

Baust, J. G. and Lee, R. E. (1981). Divergent mechanisms of frost-hardiness in two populations of the gall fly, *Eurosta solidaginis*. *J. Insect Physiol.* **27**, 485-490.

Baust, J. G. and Nishino, M. (1991). Freezing tolerance in the goldenrod gall fly (*Eurosta solidaginis*). In *Insects at Low Temperature* (ed. R. E. Lee and D. L. Denlinger), pp. 260-275. New York: Chapman and Hall.

Beitz, E. (2000). T_EXtopo: shaded membrane protein topology plots in LAT_EX2_ε. *Bioinformatics* **16**, 1050-1051.

Bennett, V. A. and Lee, R. E. (1997). Modeling seasonal changes in intracellular freeze-tolerance of fat body cells of the gall fly, *Eurosta solidaginis* (Diptera: Tephritidae). *J. Exp. Biol.* **200**, 185-192.

Bennett, V. A., Pruitt, N. L. and Lee, R. E. (1997). Seasonal changes in fatty acid composition associated with cold-hardening in third instar larvae of *Eurosta solidaginis*. *J. Comp. Physiol. B* **167**, 249-255.

Borgnia, M., Nielsen, S., Engel, A. and Agre, P. (1999). Cellular and molecular biology of the aquaporin water channels. *Annu. Rev. Biochem.* **68**, 425-458.

Bossi, E., Fabbrini, M. S. and Ceriotti, A. (2007). Exogenous protein expression in *Xenopus* oocytes: Basic procedures. In *Methods in Molecular Biology*, vol. 375, *In Vitro Transcription and Translation Protocols*, 2nd edn (ed. G. Grandi), pp. 107-131. Totowa, NJ, USA: Humana Press Inc.

Campbell, E. M., Ball, A., Hoppler, S. and Bowman, A. (2008). Invertebrate aquaporins: A review. *J. Comp. Physiol. B* **178**, 935-955.

Carlson, S. D., Juang, J.-L., Hilgers, S. L. and Garment, M. B. (2000). Blood barriers of insects. *Annu. Rev. Entomol.* **45**, 151-174.

Carpenter, J. F. and Crowe, J. H. (1988). The mechanisms of cryoprotection of proteins by solutes. *Cryobiology* **25**, 244-255.

Chapman, R. F. (1971). *The Insects: Structure and Function*. New York: Elsevier North Holland.

Collins, S. D., Allenspach, A. and Lee, R. E. (1997). Ultrastructural effects of lethal freezing on brain, muscle and Malpighian tubules from freeze-tolerant larvae of the gall fly, *Eurosta solidaginis*. *J. Insect Physiol.* **43**, 39-45.

Costanzo, J. P., Lee, R. E. and Wright, M. F. (1991). Effect of cooling rate on the survival of frozen wood frogs, Rana sylvatica. *J. Comp. Physiol. B* **161**, 225-229.
Davis, D. J. and Lee, R. E. (2001). Intracellular freezing, viability, and composition of fat body cells from freeze-intolerant larvae of *Sarcophaga crassipalpis*. *Arch. Insect Biochem.* **48**, 199-205.
De Castro, E., Sigrist, C. J. A., Gattiker, A., Bulliard, V., Langendijk-Genevaux, P. S., Gasteiger, E., Bairoch, A. and Hulo, N. (2006). ScanProsite: Detection of PROSITE signature matches and ProRule-associated functional and structural residues in proteins. *Nucleic Acids Res.* **1**, 362-365.
Echevarria, M., Windhager, E. E. and Frindt, G. (1996). Selectivity of the renal collecting duct water channel aquaporin-3. *J. Biol. Chem.* **271**, 25079-25082.
Echevarria, M., Ramirez-Lorca, R., Hernandez, C. S., Gutierriez, A., Mendez-Ferrer, S., Gonzalez, E., Toledo-Aral, J. J., Ilundain, A. A. and Whittembury, G. (2001). Identification of a new water channel (Rp-MIP) in the Malpighian tubules of the insect *Rhodnius prolixus*. *Pflugers Arch.* **442**, 27-34.
Edashige, K., Yamaji, Y., Kleinhans, F. W. and Kasai, M. (2003). Artificial expression of aquaporin-3 improves the survival of mouse oocytes after cryopreservation. *Biol. Reprod.* **68**, 87-94.
Elvin, C. M., Bunch, R., Liyou, N. E., Pearson, R. D., Gough, J. and Drinkwater, R. D. (1999). Molecular cloning and expression in *Escherichia coli* of an aquaporin-like gene from adult buffalo fly (*Haematobia irritans exigua*). *Insect Mol. Biol.* **8**, 369-380.
Hadley, N. F. (1994). *Water Relations of Terrestrial Arthropods.* New York: Academic Press.
Hall, B. G. (2004). *Phylogenetic Trees Made Easy: A How-to Manual.* Massachusetts: Sinauer Associates.
Hall, T. (1999). BioEdit: a user friendly biological sequence alignment editor and analysis program for Windows 95/98/NT. *Nucleic Acids Symp. Ser.* **41**, 95-98.
Hinton, H. E. (1960). A fly larva that tolerates dehydration and temperatures of –270° to +102°C. *Nature* **188**, 336-337.
Holland, L. Z., McFall-Ngai, M. and Somero, G. N. (1997). Evolution of lactate dehydrogenase-A homologs of barracuda fishes (Genus *Sphyraena*) from different thermal environments: Differences in kinetic properties and thermal stability are due to amino acid substitutions outside the active site. *Biochemistry* **36**, 3207-3215.
Humphrey, W., Dalke, A. and Schulten, K. (1996). VMD-Visual Molecular Dynamics. *J. Mol. Graph.* **14**, 33-38.
Irwin, J. T., Bennett, V. A. and Lee, R. E. (2001). Diapause development in frozen larvae of the goldenrod gall fly, *Eurosta solidaginis* Fitch (Diptera: Tephritidae). *J. Comp. Physiol. B* **171**, 181-188.
Izumi, Y., Sonoda, S., Yoshida, H., Danks, H. V. and Tsumuki, H. (2006). Role of membrane transport of water and glycerol in the freeze tolerance of the rice stem borer, *Chilo suppressalis* Walker (Lepidoptera: Pyralidae). *J. Insect Physiol.* **52**, 215-220.
Karow, A. M. (1991). Chemical cryoprotection of metazoan cells. *Bioscience* **41**, 155-160.
Kataoka, N., Miyake, S. and Azuma, M. (2009). Aquaporin and aquaglyceroporin in silkworms, differently expressed in the hindgut and midgut of *Bombyx mori*. *Insect Mol. Biol.* **18**, 303-314.
Kikawada, T., Saito, A., Kanamori, Y., Fujita, M., Snigorska, K., Watanabe, M. and Okuda, T. (2008). Dehydration-inducible changes in expression of two aquaporins in the sleeping chironomid, *Polypedilum vanderplanki*. *Biochim. Biophys. Acta* **1778**, 514-520.
Kukal, O., Serianni, A. S. and Duman, J. G. (1988). Glycerol metabolism in a freeze-tolerant arctic insect: An *in vivo* ^{13}C NMR study. *J. Comp. Physiol. B* **158**, 175-183.
Kumar, S., Dudley, J., Nei, M. and Tamura, K. (2008). MEGA: A biologist-centric software for evolutionary analysis of DNA and protein sequences. *Brief. Bioinform.* **9**, 299-306.
Kyte, J. and Doolittle, R. F. (1982). A simple method for displaying the hydropathic character of a protein. *J. Mol. Biol.* **157**, 105-132.
Layne, J. R. (1993). Winter microclimate of goldenrod spherical galls and its effects on the gall inhabitant *Eurosta solidaginis* (Diptera: Tephritidae). *J. Therm. Biol.* **18**, 125-130.
Le Caherec, F., Deschamps, S., Delamarche, C., Pellerin, I., Bonnec, G., Guillam, M., Thomas, D., Gouranton, J. and Hubert, J. (1996). Molecular cloning and characterization of an insect aquaporin: Functional comparison with aquaporin 1. *Eur. J. Biochem.* **241**, 707-715.
Lee, R. E. (1991). Principles of insect low temperature tolerance. In *Insects at Low Temperature* (ed. R. E. Lee and D. L. Denlinger), pp. 17-46. New York: Chapman and Hall.
Lee, R. E. (2010). A primer on insect cold-tolerance. In *Low Temperature Biology of Insects* (ed. D. L. Denlinger and R. E. Lee), pp. 3-34. New York: Cambridge University Press.
Lee, R. E., McGrath, J. J., Morason, R. T. and Taddeo, R. M. (1993). Survival of intracellular freezing, lipid coalescence and osmotic fragility in fat-body cells of the freeze-tolerant gall fly *Eurosta solidaginis*. *J. Insect Physiol.* **39**, 445-450.
Mazur, P. (1984). Freezing of living cells: Mechanisms and implication. *Am. J. Physiol.* **247**, 125-142.
Morrissey, R. E. and Baust, J. G. (1976). The ontogeny of cold tolerance in the gall fly, *Eurosta solidaginis*. *J. Insect Physiol.* **22**, 431-437.
Muldrew, K., Acker, J. P., Elliot, J. A. W. and McGann, L. E. (2004). The water to ice transition: Implications for living cells. In *Life in the Frozen State* (ed. B. J. Fuller, N. Lane and E. E. Benson), pp. 67-108. New York: CRC Press.
Nylander, J. A. A. (2004). MrModeltest v.2. Program distributed by the author. Evolutionary Biology Centre, Uppsala University (http://www.abc.se/~nylander/mrmodeltest2/mrmodeltest2.html).
Papadopoulos, M. C. and Verkman, A. S. (2007). Aquaporin-4 and brain edema. *Pedriatr. Nephrol.* **22**, 778-784.
Papadopoulos, M. C., Manley, G. T., Krishna, S. and Verkman, A. S. (2004). Aquaporin-4 facilitates reabsorption of excess fluid in vasogenic brain edema. *FASEB J.* **18**, 1291-1293.
Philip, B. N. and Lee, R. E. (2010). Changes in abundance of aquaporin-like proteins occurs concomitantly with seasonal acquisition of freeze tolerance in the goldenrod gall fly, *Eurosta solidaginis*. *J. Insect Physiol.* **56**, 679-685.
Philip, B. N., Yi, S.-X., Elnitsky, M. A. and Lee, R. E. (2008). Aquaporins play a role in desiccation and freeze tolerance in larvae of the goldenrod gall fly, *Eurosta solidaginis*. *J. Exp. Biol.* **211**, 1114-1119.
Preston, G. M., Carroll, T. P., Guggino, W. B. and Agre, P. (1992). Appearance of water channels in *Xenopus* oocytes expressing red cell CHIP28 protein. *Science* **256**, 385-387.
Preston, G. M., Jung, J. S., Guggino, W. B. and Agre, P. (1993). The mercury-sensitive residue at cysteine 189 in the CHIP28 water channel. *J. Biol. Chem.* **268**, 17-20.
Ring, R. A. and Danks, H. V. (1994). Desiccation and cryoprotection: Overlapping adaptations. *Cryo Letters* **15**, 181-190.
Rojas, R. R., Lee, R. E. and Baust, J. G. (1986). Relationship of environmental water content to glycerol accumulation in the freezing tolerant larvae of *Eurosta solidaginis* (Fitch). *Cryo Letters* **7**, 234-245.
Sambrook, J. and Russell, D. W. (2001). *Molecular Cloning: A Laboratory Manual*, 3rd edn. New York: Cold Spring Harbor Laboratory Press.
Shakesby, A. J., Wallace, I. S., Isaacs, H. V., Pritchard, J., Roberts, D. M. and Douglas, A. E. (2009). A water-specific aquaporin involved in aphid osmoregulation. *Insect Biochem. Mol. Biol.* **39**, 1-10.
Simmons, M. P., Ochoterena, H. and Freudenstein, J. V. (2002). Amino acid vs. nucleotide characters: Challenging preconceived notions. *Mol. Phylogenet. Evol.* **24**, 78-90.
Tait, M. J., Saadoun, S., Bell, B. A. and Papadopoulos, M. C. (2008). Water movements in the brain: Role of aquaporins. *Trends Neurosci.* **31**, 37-43.
Tanghe, A., Van Dijck, P., Dumortier, F., Teunissen, A., Hohmann, S. and Thevelein, J. M. (2002). Aquaporin expression correlates with freeze tolerance in baker's yeast, and overexpression improves freeze tolerance in industrial strains. *Appl. Environ. Microbiol.* **68**, 5981-5989.
Waddell, P. J. and Steel, M. A. (1997). General time-reversible distances with unequal rates across sites: mixing gamma and inverse Gaussian distributions with invariant sites. *Mol. Phylogenet. Evol.* **8**, 398-414.
Zhang, R. and Verkman, A. S. (1991). Water and urea permeability properties of *Xenopus* oocytes: Expression of mRNA from toad urinary bladder. *Am. J. Physiol.* **260**, 26-34.
Zimmerman, S. L., Frisbie, J., Goldstein, D. L., West, J., Rivera, K. and Krane, C. M. (2007). Excretion and conservation of glycerol, and expression of aquaporins and glyceroporins, during cold acclimation in Cope's gray tree frog *Hyla chrysoscelis*. *Am. J. Physiol.* **292**, 544-555.